

Prospects for Quarkonium Physics at HERA

Matteo Cacciari and Michael Krämer

Deutsches Elektronen-Synchrotron DESY, D-22607 Hamburg, FRG

Abstract: We work out and review prospects for future quarkonium physics at HERA. We focus on the impact of color-octet contributions and discuss how measurements at HERA can be used to test the picture of quarkonium production as developed in the context of the NRQCD factorization approach.

1 Introduction

The production of heavy quarkonium states in high energy collisions provides an important tool to study the interplay between perturbative and nonperturbative QCD dynamics. Quarkonium production in deep inelastic scattering and photon-proton collisions at HERA has been analysed at some length in the context of the previous HERA workshops (see e.g. ref.[1]). However, most of the previous studies have been carried out within the color-singlet model (CSM) [2] or the color-evaporation model [3]. Only recently, a rigorous theoretical framework for treating quarkonium production and decays has been developed in ref.[4]. The factorization approach is based on the use of non-relativistic QCD (NRQCD) [5] to separate the short-distance parts from the long-distance matrix elements and explicitly takes into account the complete structure of the quarkonium Fock space. This formalism implies that so-called color-octet processes, in which the heavy-quark antiquark pair is produced at short distances in a color-octet state and subsequently evolves nonperturbatively into a physical quarkonium, should contribute to the cross section. According to the factorization formalism, the inclusive cross section for the production of a quarkonium state H can be expressed as a sum of terms, each of which factors into a short-distance coefficient and a long-distance matrix element:

$$d\sigma(ep \rightarrow H + X) = \sum_n d\hat{\sigma}(ep \rightarrow Q\bar{Q}[n] + X) \langle \mathcal{O}^H[n] \rangle. \quad (1)$$

Here, $d\hat{\sigma}$ denotes the short-distance cross section for producing an on-shell $Q\bar{Q}$ -pair in a color, spin and angular-momentum state labelled by n . The NRQCD vev matrix elements $\langle \mathcal{O}^H[n] \rangle$ give the probability for a $Q\bar{Q}$ -pair in the state n to form the quarkonium state

H . The relative importance of the various terms in (1) can be estimated by using NRQCD velocity scaling rules [6]. For $v \rightarrow 0$ (v being the average velocity of the heavy quark in the quarkonium rest frame) each of the NRQCD matrix elements scales with a definite power of v and the general expression (1) can be organized into an expansion in powers of v^2 .

It has recently been argued in refs.[7, 8] that quarkonium production in hadronic collisions at the Tevatron can be accounted for by including color-octet processes and by adjusting the unknown long-distance color-octet matrix elements to fit the data. In order to establish the phenomenological significance of the color-octet mechanism it is however necessary to identify color-octet contributions in different production processes.¹ In this report we will focus our discussion on the prospects of extracting information on the color-octet processes from the measurements of inelastic quarkonium production at HERA. Elastic/diffractive mechanisms will be discussed elsewhere [10]. We shall briefly review the impact of color-octet contributions and higher-order QCD corrections on the cross section for J/ψ photoproduction and compare the theoretical predictions with recent experimental data. In this context we will also comment on the possibility of measuring the gluon distribution in the proton from J/ψ photoproduction. The high-statistics data to be expected in the future at HERA will allow for a detailed comparison of the theoretical predictions with experimental data not only for J/ψ photoproduction, but also for various other channels and final states, like photoproduction of ψ' , Υ and χ states, associated $J/\psi + \gamma$ production, fragmentation and resolved-photon contributions as well as deep inelastic J/ψ production. We will discuss how these reactions can be used to constrain the color-octet matrix elements and test the picture of quarkonium production as developed in the context of the NRQCD factorization approach.

2 J/ψ photoproduction

Quarkonium production in high energy ep collisions at HERA is dominated by photoproduction events where the electron is scattered by a small angle producing photons of almost zero virtuality. The measurements at HERA provide information on the dynamics of quarkonium photoproduction in a wide kinematical region, $30 \text{ GeV} \lesssim \sqrt{s_{\gamma p}} \lesssim 200 \text{ GeV}$, corresponding to initial photon energies in a fixed-target experiment of $450 \text{ GeV} \lesssim E_\gamma \lesssim 20,000 \text{ GeV}$. The production of J/ψ particles in photon-proton collisions proceeds predominantly through photon-gluon fusion. Elastic/diffractive mechanisms can be eliminated by measuring the J/ψ energy spectrum, described by the scaling variable $z = p \cdot k_\psi / p \cdot k_\gamma$, with $p, k_{\psi, \gamma}$ being the momenta of the proton and $J/\psi, \gamma$ particles, respectively. In the

¹Quarkonium production via color-octet states has also been studied in e^+e^- annihilation and Z decays, for hadronic collisions in the energy range of fixed-target experiments and in B decays [9].

proton rest frame, z is the ratio of the J/ψ to γ energy, $z = E_\psi/E_\gamma$. For elastic/diffractive events z is close to one; a clean sample of inelastic events can be obtained in the range $z \lesssim 0.9$.

For J/ψ production and at leading order in v^2 , the general factorization formula (1) reduces to the standard expression of the color-singlet model [2]. The short-distance cross section is given by the subprocess

$$\gamma + g \rightarrow c\bar{c} [{}^3S_1, \underline{1}] + g \quad (2)$$

with $c\bar{c}$ in a color-singlet state (denoted by $\underline{1}$), zero relative velocity, and spin/angular-momentum quantum numbers ${}^{2S+1}L_J = {}^3S_1$. Relativistic corrections due to the motion of the charm quarks in the J/ψ bound state enhance the large- z region, but can be neglected in the inelastic domain [11]. The calculation of the higher-order perturbative QCD corrections to the short-distance process (2) has been performed in refs.[12, 13]. Inclusion of the NLO corrections reduces the scale dependence of the theoretical prediction and increases the color-singlet cross section by more than 50%, depending in detail on the photon-proton energy and the choice of parameters [13].

Color-octet configurations are produced at leading order in α_s through the $2 \rightarrow 1$ parton processes [14, 15, 16]

$$\begin{aligned} \gamma + g &\rightarrow c\bar{c} [{}^1S_0, \underline{8}] \\ \gamma + g &\rightarrow c\bar{c} [{}^3P_{0,2}, \underline{8}] . \end{aligned} \quad (3)$$

Due to kinematical constraints, the leading color-octet terms will only contribute to the upper endpoint of the J/ψ energy spectrum, $z \approx 1$ and $p_T \approx 0$, p_T being the J/ψ transverse momentum. It has, however, been argued in ref.[17] that sizable higher-twist effects are expected to contribute in the region $p_T \lesssim 1$ GeV, which cause the breakdown of the factorization formula (1). Moreover, diffractive production mechanisms which cannot be calculated within perturbative QCD might contaminate the region $z \approx 1$ and make it difficult to extract precise information on the color-octet processes.

It is therefore more appropriate to study J/ψ photoproduction in the inelastic region $z \leq 0.9$ and $p_T \geq 1$ GeV where no diffractive channels contribute and where the general factorization formula (1) and perturbative QCD calculations should be applicable. Color-octet configurations which contribute to inelastic J/ψ photoproduction are produced through the subprocesses [14, 16]

$$\begin{aligned} \gamma + g &\rightarrow c\bar{c} [{}^1S_0, \underline{8}] + g \\ \gamma + g &\rightarrow c\bar{c} [{}^3S_1, \underline{8}] + g \\ \gamma + g &\rightarrow c\bar{c} [{}^3P_{0,1,2}, \underline{8}] + g . \end{aligned} \quad (4)$$

Light-quark initiated contributions are strongly suppressed at HERA energies and can safely be neglected. Adopting NRQCD matrix elements consistent with those extracted from the fits to prompt J/ψ data at the Tevatron [8] (see Table 1) one finds that color-octet and color-singlet contributions to the inelastic cross section are predicted to be

$\langle \mathcal{O}^{J/\psi} [{}^3S_1, \underline{1}] \rangle$	1.16 GeV ³	$m_c^3 v^3$
$\langle \mathcal{O}^{J/\psi} [{}^1S_0, \underline{8}] \rangle$	10^{-2} GeV ³	$m_c^3 v^7$
$\langle \mathcal{O}^{J/\psi} [{}^3S_1, \underline{8}] \rangle$	10^{-2} GeV ³	$m_c^3 v^7$
$\langle \mathcal{O}^{J/\psi} [{}^3P_0, \underline{8}] \rangle / m_c^2$	10^{-2} GeV ³	$m_c^3 v^7$

Table 1: Values of the NRQCD matrix elements used in the numerical analysis, with the velocity and mass scaling. v is the velocity of the heavy quark in the quarkonium rest frame. For charmonium it holds $v^2 \simeq 0.25$.

of comparable size [14, 16]. However, taking into account the uncertainty due to the value of the charm quark mass and the strong coupling, the significance of color-octet contributions can not easily be deduced from the analysis of the absolute J/ψ production rates. A distinctive signal for color-octet processes should, however, be visible in the J/ψ energy distribution $d\sigma/dz$ shown in fig.1 [8]. Since the shape of the distribution is insensitive to higher-order QCD corrections or to the uncertainty induced by the choice for m_c and α_s , the analysis of the J/ψ energy spectrum $d\sigma/dz$ should provide a clean test for the underlying production mechanism. From fig.1 we can conclude that the shape predicted by the color-octet contributions is not supported by the experimental data and that the J/ψ energy spectrum is adequately accounted for by the color-singlet channel. This is however not to be considered as a failure of the factorization approach, since also other analyses (see for instance the last item of ref. [9]) have pointed out that the fits to the Tevatron data may have returned slightly too large values for the matrix elements. With higher statistics data it will be possible to extract more detailed information on the color-octet matrix elements, in particular from the analysis of the J/ψ energy distribution in the inelastic region.

The impact of higher-order QCD corrections on total cross sections and differential distributions has been studied thoroughly for the color-singlet channel in ref.[13]. A detailed analysis of the spectra in the high energy range at HERA shows that the perturbative calculation is not well-behaved in the limit $p_T \rightarrow 0$, where p_T is the transverse momentum of the J/ψ . No reliable prediction can be made in this singular boundary region without resummation of large logarithmic corrections caused by multiple gluon emission. If the small p_T region is excluded from the analysis, experimental results on differential distributions and total cross sections are well accounted for by the color-singlet channel alone,

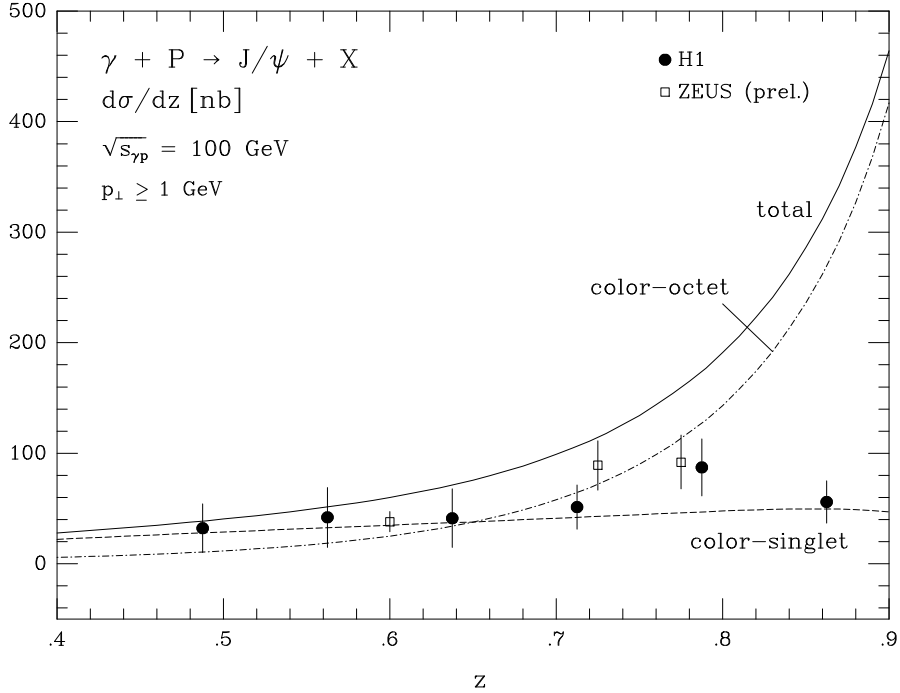


Figure 1: Color-singlet and color-octet contributions to the J/ψ energy distribution $d\sigma/dz$ at the photon-proton centre of mass energy $\sqrt{s_{\gamma p}} = 100$ GeV integrated in the range $p_T \geq 1$ GeV [14]. Experimental data from [18, 19].

including NLO QCD corrections, see e.g. fig.2. However, since the average momentum fraction of the partons is shifted to larger values when excluding the small- p_T region, the sensitivity of the prediction to the small- x behaviour of the gluon distribution is not very distinctive. A detailed analysis reveals that the size of the QCD corrections increases when adopting parton densities with flatter gluons. The sensitivity to different gluon distributions is thus reduced in next-to-leading order as compared to the leading-order result, in particular when choosing a small charm mass and a large value for the strong coupling. Parametrizations with extremely flat gluons like MRS(D0') [21] are clearly disfavoured by the recent HERA measurements of the proton structure function [22] and do not allow for a reliable prediction in the high energy region. For the parameters adopted in fig.2, the MRS(D0') distribution leads to next-to-leading order results not very different from those obtained with the MRS(A') parametrization. The corresponding K -factors are however uncomfortably large, $K \sim 4$, casting doubts on the reliability of the perturbative expansion as obtained by using flat gluon distributions. If parton distributions with steep gluon densities are adopted, the next-to-leading order cross section is well-behaved and gives an adequate description of the experimental data, as demonstrated in fig.2.

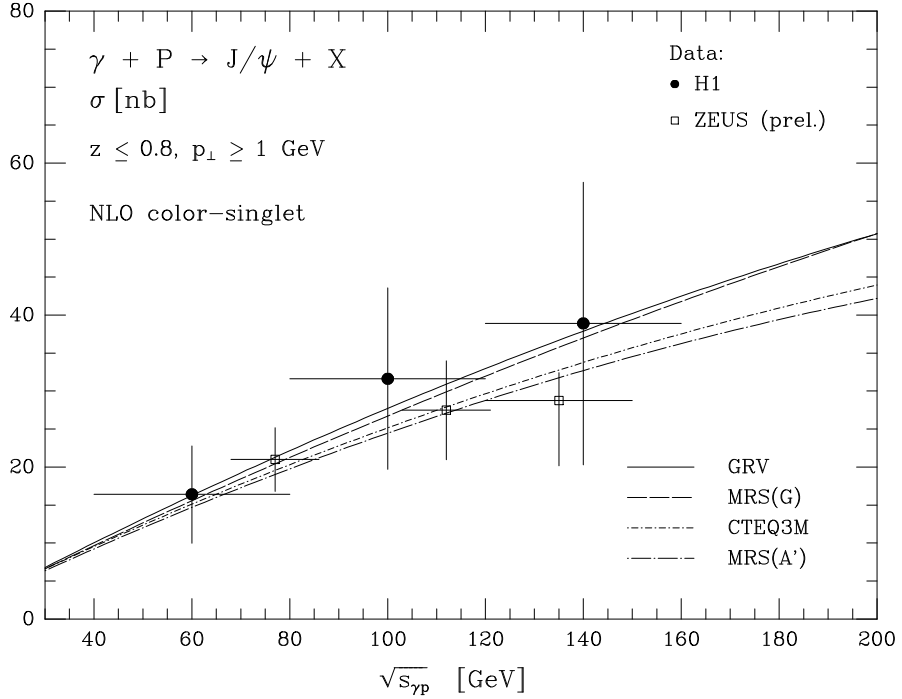


Figure 2: NLO color-singlet prediction for the total inelastic J/ψ photoproduction cross section as a function of the photon-proton energy for different parametrizations [20] of the parton distribution in the proton [13]. Experimental data from [18, 19].

The cross section for the production of ψ' particles has been measured by several photo- and hadroproduction experiments [23] to be suppressed by a factor ~ 0.25 compared to J/ψ production. This result is consistent with naive estimates obtained within the color-singlet model where one assumes that the effective charm masses in the short distance amplitudes scale like the corresponding ψ' and J/ψ masses [2]. Within the NRQCD factorization approach it is however conceptually preferred to express the short-distance coefficients in terms of the charm quark mass rather than the quarkonium mass, yielding $\sigma(\psi')/\sigma(J/\psi) \sim 0.5$ for color-singlet dominated production channels. Relativistic corrections and color-octet contributions are expected to affect the ratio $\sigma(\psi')/\sigma(J/\psi)$, but no quantitative prediction can be made with the present experimental and theoretical information.

Bottomonium production is a particular interesting subject to be studied at HERA. The larger value of the bottom quark mass makes the perturbative QCD predictions of the short-distance cross section more reliable than for charm production. Moreover, the derivation of the factorization formula eq.(1) relies on the fact that the momentum scales which govern the bound state dynamics are well separated: $(m_Q v^2)^2 \ll (m_Q v)^2 \ll m_Q^2$. This assumption is reasonably good for charmonium (where $v^2 \sim 0.3$) but very good

for bottomonium (where $v^2 \sim 0.1$). Thus, the theoretical predictions for bottomonium production should be much more reliable than those for charmonium. The production rates for Υ bound states are, however, suppressed, compared with J/ψ states, by a factor of about 300 at HERA, a consequence of the smaller bottom electric charge and the phase space reduction by the large b mass.

3 J/ψ production via fragmentation

At sufficiently large transverse momentum p_T , quarkonia production is dominated by fragmentation, the production of a parton with large p_T which subsequently decays into the quarkonium state and other partons [24]. While the fragmentation contributions are of higher order in α_s compared to direct quarkonia production in fusion processes, they are enhanced by powers p_T^2/m_c^2 and can thus overtake the fusion contribution at $p_T \gg m_c$. It has in fact been argued that quarkonium production at large p_T in hadronic collisions at the Tevatron can be accounted for by including gluon fragmentation into color-octet states [7].

The fragmentation contribution to the differential cross section for producing a quarkonium state H at large p_T can be written in the factorized form

$$d\sigma(\gamma + p \rightarrow H + X) = \sum_i \int_0^1 d\zeta d\hat{\sigma}(\gamma + p \rightarrow i + X) D_{i \rightarrow H}(\zeta) \quad (5)$$

where $d\hat{\sigma}$ is the differential cross section for producing a parton of type i with momentum p_T/ζ . The fragmentation function $D_{i \rightarrow H}$ gives the probability that a jet initiated by parton i contains a hadron H carrying a fraction ζ of the parton momentum. According to the NRQCD factorization formalism, fragmentation functions for charmonium have the general form

$$D_{i \rightarrow H}(\zeta, \mu) = \sum_n d_{i \rightarrow c\bar{c}[n]X}(\zeta, \mu) \langle \mathcal{O}^H[n] \rangle \quad (6)$$

analogous to eq.(1). The function $d_{i \rightarrow c\bar{c}[n]X}$ gives the probability for the parton i to form a jet that includes a $c\bar{c}$ pair in the state labelled by n . It can be calculated at an initial scale $\mu \sim m_c$ as a perturbative expansion in $\alpha_s(m_c)$ [24, 25] and be evolved up to higher scales $\mu \sim p_T$ by using the Altarelli-Parisi evolution equations.

A quantitative analysis of the fragmentation contributions to J/ψ photoproduction at HERA has been performed in ref.[26] (see also ref.[27] for an earlier analysis within the color-singlet model). The authors have considered the fragmentation of gluons and charm quarks produced at leading order via the Compton- and Bethe-Heitler processes, $\gamma + q \rightarrow q + g$ and $\gamma + g \rightarrow c + \bar{c}$, respectively. It appears that at large transverse momenta, $p_T \gtrsim 10$ GeV, color-singlet charm quark fragmentation dominates over the photon-gluon

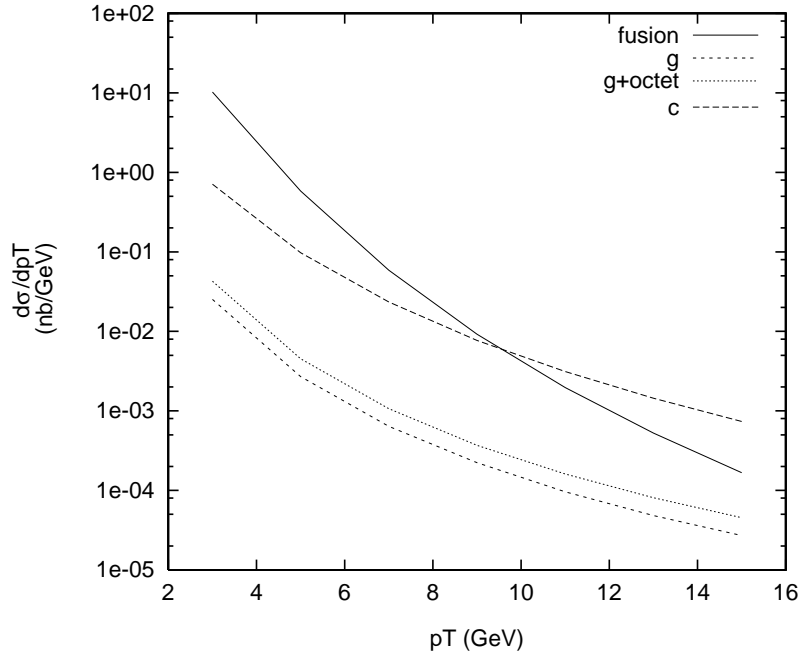


Figure 3: Transverse momentum distribution $d\sigma/dp_T$ for J/ψ photoproduction at the photon-proton centre of mass energy $\nu = 100$ GeV. The solid line represents the (leading-order) fusion contribution and the dashed-dotted line the charm quark fragmentation contribution. The dotted and dashed lines represent the gluon fragmentation contributions with and without a color-octet component for the S state. The cut on the inelasticity parameter z is $0.1 < z < 0.9$. From Ref.[26].

fusion process while gluon-fragmentation is suppressed by an order of magnitude over the whole range of p_T , see fig.3 [26]. Color-octet contributions to the gluon fragmentation function considerably enhance the large- z region, but have no strong effect in the inelastic domain $z \lesssim 0.9$. Thus, the information that will be obtained from large p_T production of J/ψ particles at HERA can be used to study the charm quark fragmentation mechanism and is complementary to the analyses performed at the Tevatron where the large p_T region is dominated by gluon fragmentation. However, since the cross section for J/ψ photoproduction at $p_T \gtrsim 10$ GeV is at the most $\mathcal{O}(1\text{pb})$, a large luminosity is required to probe fragmentation contributions to quarkonium production at HERA.

4 Resolved photon contributions

The photoproduction of a J/ψ particle can also take place via a so called resolved photon interaction, where the photon couples through one of its hadronic components. For J/ψ

production within the color-singlet model the process goes like:

$$\gamma p \rightarrow g_\gamma + g_p \rightarrow c\bar{c}[{}^3S_1, \underline{1}] + g \rightarrow J/\psi + g \quad (7)$$

meaning that the gluon coming from the photon fuses with the one coming from the proton to give a 3S_1 color-singlet $c\bar{c}$ pair which subsequently hadronizes into a J/ψ . This process has been extensively analyzed in the past (see for instance [1]) and found to contribute to the overall cross section only marginally everywhere but in the low- z region. More contributions, coming from production and radiative decay of χ states, are also expected to be present. These terms also probe the quark content of the photon. They are expected to be of comparable size with the J/ψ production process (7) described above (see [1] for a survey of these and other resolved production mechanisms).

Within the factorization approach, however, more channels have to be considered, where the J/ψ production goes via color-octet $c\bar{c}$ pairs. Namely, the following processes contribute:

$$\begin{aligned} g_\gamma + g_p &\rightarrow c\bar{c}[{}^1S_0, \underline{8}] + g \\ g_\gamma + g_p &\rightarrow c\bar{c}[{}^3S_1, \underline{8}] + g \\ g_\gamma + g_p &\rightarrow c\bar{c}[{}^3P_J, \underline{8}] + g. \end{aligned}$$

They are in every respect analogous to the ones which have been argued to greatly increase the J/ψ production in $p\bar{p}$ collisions at the Tevatron. They must therefore be carefully considered here to understand whether or not they change the picture established by the CSM.

Using the matrix elements squared evaluated in ref.[8] and the choice of nonperturbative parameters displayed in Table 1 we can calculate the cross sections and compare them with the CSM ones. The results are shown in Table 2, with a minimum p_T cut needed to screen the collinear singularity present in the 1S_0 and 3P_J channels.

These results make clear that the color-octet channels could provide a non-negligible increment of the overall J/ψ photoproduction cross section. It's therefore worth studying in more detail which regions of phase space will be mostly affected. A close look to the differential distributions of experimental interest shows that the behaviour of the color-octet contributions to the resolved channels is similar to that of the color-singlet one. Namely, it is only visible in the low- z region. Fig.4 shows the z distribution for the direct photon color-singlet channel (full line) compared with the old CSM resolved photon contribution (dashed line) and the new resolved photon color-octet one (dotted line). The resolved contributions can be seen to be enhanced by the color-octet terms, but the qualitative picture of them being visible only in the low- z region remains unchanged.

Channel		$\sigma_{\gamma p}$ (nb) $\sqrt{s} = 100$ GeV $p_T > 1$ GeV
Direct	$^3S_1, \underline{1}$	13.68
Resolved	$^3S_1, \underline{1}$.48
	$^1S_0, \underline{8}$.79
	$^3S_1, \underline{8}$.34
	$^3P_0, \underline{8}$	1.61
	$^3P_1, \underline{8}$.50
	$^3P_2, \underline{8}$	2.06

Table 2: Results for the total cross sections (in nb).

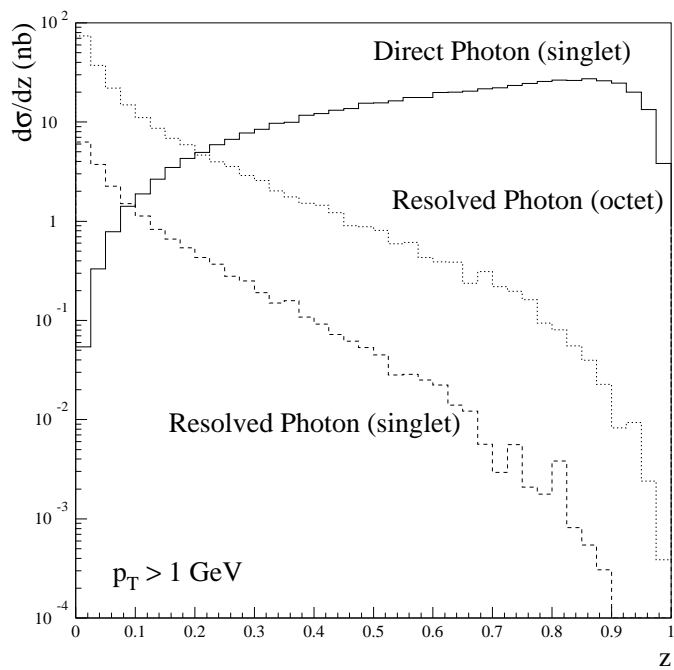


Figure 4: Comparison of the inelasticity distributions for direct (singlet) and resolved (singlet and octet) J/ψ photoproduction.

5 χ photoproduction

For the production of S -wave quarkonia, like J/ψ , ψ' or Υ , the factorization approach coincides with the color-singlet model in the nonrelativistic limit $v \rightarrow 0$. In the case of χ bound states, however, color-singlet and color-octet mechanisms contribute at the same order in v to annihilation rates and production cross sections and must therefore both be included for a consistent calculation [28]. The production of χ states plays a peculiar role

in photon-hadron collisions. Unlike what happens in hadron-hadron collisions, were χ s are copiously produced by gg , gq and $q\bar{q}$ interactions, the process

$$\gamma + g \rightarrow c\bar{c}[^3P_J, \underline{1}] + g \quad (8)$$

namely the production of a color-singlet $c\bar{c}$ pair with the χ quantum numbers, happens to be forbidden at leading order in α_s . This is due to the color factor of the two gluons having to be symmetric in order to produce a color-singlet states. The gluons could therefore be replaced by two colorless photons, and the process $\chi \rightarrow \gamma\gamma\gamma$ is known to be forbidden by the request of charge conjugation invariance.

To have χ production initiated by a direct photon we must therefore either go to higher orders within the CSM, adding one gluon to the leading order diagram, or consider color-octet mediated channels.

Within the factorization approach, indeed, χ production can still take place at the leading $\mathcal{O}(\alpha\alpha_s^2)$, provided it is a color-octet 3S_1 charm pair which is produced in the hard interaction and subsequently hadronizes into a physical χ particle. The following two processes contribute:

$$\begin{aligned} \gamma + g &\rightarrow c\bar{c}[{}^3S_1, \underline{8}] + g \\ \gamma + q(\bar{q}) &\rightarrow c\bar{c}[{}^3S_1, \underline{8}] + q(\bar{q}) \end{aligned}$$

The first of these two reaction is by far the dominant one in the HERA energy range and at low transverse momentum. Within the spirit of the factorization approach, the cross section is given by the same short distance cross section evaluated for color-octet J/ψ photoproduction (see eq.(1) and the second process of eq.(4)), times the appropriate matrix elements $\langle \mathcal{O}^{\chi_J}[{}^3S_1, \underline{8}] \rangle$. These matrix elements have also been fitted to the Tevatron data in [7, 8], and found to be of order 10^{-2} GeV 3 . Using, for the sake of simplicity, $\langle \mathcal{O}^{\chi_0}[{}^3S_1, \underline{8}] \rangle = 10^{-2}$ GeV 3 and the relation

$$\langle \mathcal{O}^{\chi_J}[{}^3S_1, \underline{8}] \rangle = (2J+1) \langle \mathcal{O}^{\chi_0}[{}^3S_1, \underline{8}] \rangle \quad (9)$$

we find

$$\sum_J \sigma(\gamma p \rightarrow \chi_J) = 9 \langle \mathcal{O}^{\chi_0}[{}^3S_1, \underline{8}] \rangle \times 0.9 \text{ nb GeV}^{-3} \simeq 80 \text{ pb} \quad (10)$$

at $\sqrt{s} = 100$ GeV and with a minimum p_T cut of 3 GeV.

It is worth noticing here a pretty large discrepancy with the result of ref.[29]. Despite using a nonperturbative matrix element about a factor of two smaller than ours, it finds $\sigma(\gamma p \rightarrow \chi_1) = 0.13$ nb, which is about a factor of five larger than our result.

6 Associated $J/\psi + \gamma$ production

A particularly distinctive experimental probe of the relevance of color-octet contributions in quarkonia production can be the observation of the exclusive process given by the associated production of a J/ψ and a photon [30]²:

$$\gamma p \rightarrow J/\psi + \gamma \quad (11)$$

Within the CSM this process can only undergo via the resolved photon channel, since at least two gluons must couple to the heavy quark line to produce a color-singlet $c\bar{c}$ pair:

$$\gamma p \rightarrow g_\gamma + g_p \rightarrow c\bar{c}[{}^3S_1, \underline{1}] + \gamma \rightarrow J/\psi + \gamma \quad (12)$$

A big suppression of the cross section, and the characteristic z distribution typical of resolved photon processes, peaked at low z , can therefore be expected.

Within the factorization approach, on the other hand, other $c\bar{c}$ states can contribute and, in particular, the reaction can now proceed also via a direct photon channel. Indeed, the following processes are now possible:

Direct photon (fig.5a):

$$\begin{aligned} \gamma + g_p &\rightarrow c\bar{c}[{}^1S_0, \underline{8}] + \gamma \\ \gamma + g_p &\rightarrow c\bar{c}[{}^3S_1, \underline{8}] + \gamma \\ \gamma + g_p &\rightarrow c\bar{c}[{}^3P_J, \underline{8}] + \gamma \end{aligned}$$

Resolved photon (fig.5b):

$$\begin{aligned} g_\gamma + g_p &\rightarrow c\bar{c}[{}^1S_0, \underline{8}] + \gamma \\ g_\gamma + g_p &\rightarrow c\bar{c}[{}^3S_1, \underline{1}] + \gamma \quad (\text{Standard CSM process}) \\ g_\gamma + g_p &\rightarrow c\bar{c}[{}^3S_1, \underline{8}] + \gamma \\ g_\gamma + g_p &\rightarrow c\bar{c}[{}^3P_J, \underline{8}] + \gamma \end{aligned}$$

Though the nonperturbative matrix elements which mediate the hadronization of the color-octet $c\bar{c}$ pairs to a J/ψ are suppressed with respect to the color-singlet one (see Table 1), we can however still expect the two following features:

- i) the production of color-octet states via a direct process - rather than a resolved one - will at least partially compensate for the smaller matrix elements. We should therefore expect an increase in the overall cross section;

²see also ref.[31] for an analysis within the color-evaporation model.

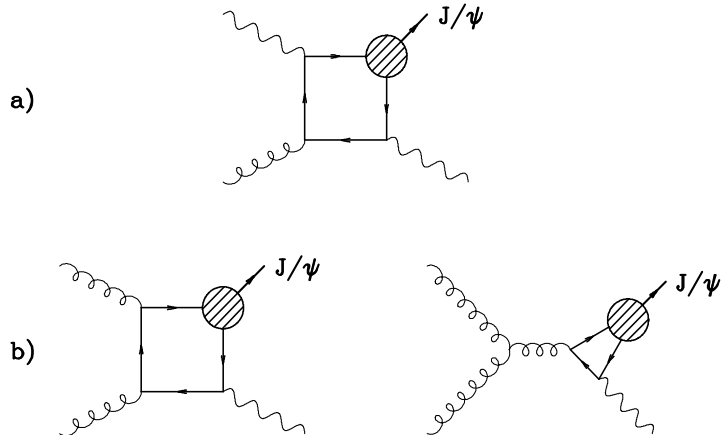


Figure 5: Diagrams contributing within the factorization approach to $J/\psi + \text{photon}$ associated production in direct (a) and resolved (b) photon collisions. In (b) the right diagram contributes to 1S_0 and 3P_J states production only.

- ii) the z distribution of the J/ψ , will be more peaked towards one. This is again due to the presence of a direct photon coupling as opposed to the resolved one, where the g_γ only carries part of the photon energy into the reaction.

These (and especially the second one) are the reasons why we expect this process to be a sensitive probe to color-octet components.

Channel		$\sigma_{\gamma p}(pb)$ $\sqrt{s} = 100 \text{ GeV}$ $p_T > 1 \text{ GeV}$
Direct	${}^1S_0, \underline{8}$	—
	${}^3S_1, \underline{8}$	7.67
	${}^3P_J, \underline{8}$	—
Resolved	${}^1S_0, \underline{8}$.35
	${}^3S_1, \underline{1}$	16.70
	${}^3S_1, \underline{8}$.27
	${}^3P_0, \underline{8}$	1.03
	${}^3P_1, \underline{8}$.14
	${}^3P_2, \underline{8}$.97

Table 3: Results for the total cross sections of $J/\psi + \gamma$ photoproduction (in pb). At leading-order, the 1S_0 and 3P_J direct contributions vanish identically.

The total cross sections (with a minimum p_T cut of 1 GeV) are shown in Table 3 for γp collisions at a cm energy of 100 GeV (see ref. [30] for more details). The bulk of the cross section can be seen to come from the standard CSM channel $gg \rightarrow c\bar{c}[^3S_1, \mathbf{1}] + \gamma$. However, the direct channel gives a non negligible contribution, amounting to about 25% of the overall cross section of ~ 27 pb. This increase is however far too small to be reliably used to assess the presence of the color-octet terms, given the smallness of this cross section (in the picobarn region) and the large theoretical uncertainties involved (like the charm mass, the strong coupling and the nonperturbative matrix elements values).

On the other hand, the study of the differential distributions can make easier to disentangle the color-octet contributions from the standard color-singlet one.

We therefore show in fig.6 the differential distributions related to the total γp cross sections at $\sqrt{s} = 100$ GeV with a minimum p_T cut of 1 GeV, presented in Table 3. The distributions due to $[^3S_1, \mathbf{1}]$ production in resolved photon collision (continuous line) and to $[^3S_1, \mathbf{8}]$ production in direct photon collision (dashed line) only are shown. The distributions due to the other color-octet processes do indeed present the same features as the ones of $[^3S_1, \mathbf{1}]$, being also produced in resolved photon interactions, but are suppressed in magnitude, as can be seen from Table 3. Their inclusion would therefore not change the picture we are going to discuss.

Fig.6 compares the result of the CSM with that due to the production of a color-octet 3S_1 state in direct photon collision, fig.5a, as predicted by the factorization approach. As expected, the effect of the direct photon coupling can easily be seen in at least some of the plots. While the p_T of the J/ψ and the invariant mass distribution of the $J/\psi\gamma$ pair are pretty similar for the two processes, the z , rapidity and photon energy distributions do indeed show a strikingly different behaviour.

Recalling that we put ourselves in the so-called “HERA-frame”, with the photon (or the electron) traveling in the direction of negative rapidities, we notice how the direct photon coupling favours the production of the quarkonium and of the photon in the negative rapidities region. This contrasts the case of resolved photon production of color-singlet 3S_1 states, which are uniformly produced around the central region.

As for the z distribution, the resolved photon process predicts a decrease of the cross section going towards the high- z region. The direct photon process does on the other hand predict the opposite behaviour: the cross section now increases going towards $z = 1$. The small dip in the last few bins is due to the minimum p_T cut.

Similarly to the z distribution behaves the photon energy one, which is predicted to be much harder in direct photon processes.

These distributions (which were also checked to be robust with respect to a higher p_T cut, so as to be sure of the absence of p_T^{min} effects) could already be good experimental

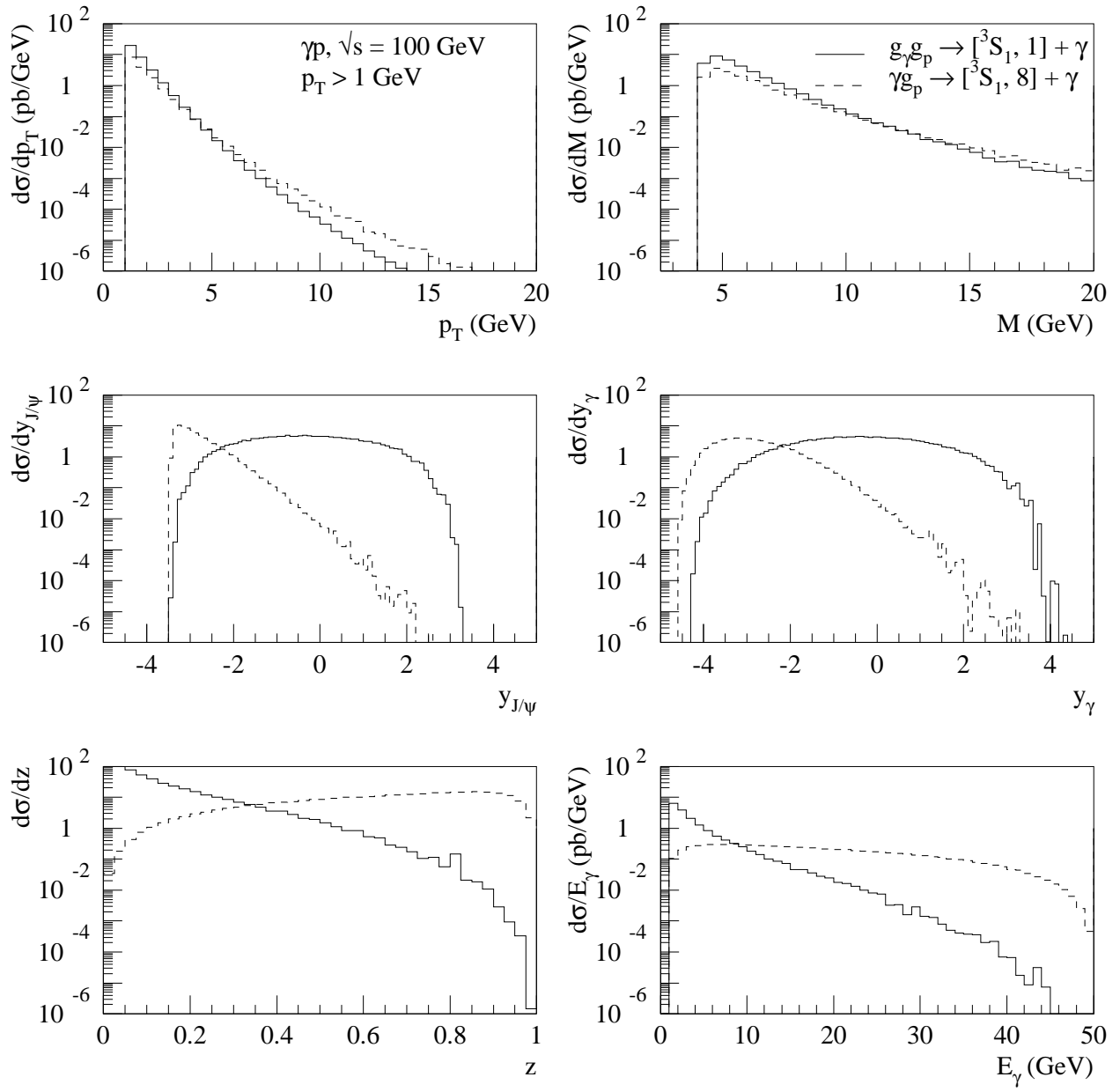


Figure 6: Differential distributions in γp collision at $\sqrt{s} = 100$ GeV. A minimum p_T cut of 1 GeV is applied.

discriminators: observation of a substantial fraction of $J/\psi + \gamma$ events in the high z region would provide good evidence for the presence of color-octet contributions to the overall cross section.

7 J/ψ production in deep inelastic scattering

Leptoproduction of quarkonium states has been extensively studied in the framework of the color-singlet model [2]. Though the color-singlet contribution can explain inelastic leptoproduction of J/ψ it can not explain the total cross section. Thus, in order to arrive at a complete description of J/ψ leptoproduction, the color-octet contributions to the J/ψ production rate have been calculated in ref.[32]. The authors obtain the following expression for the differential subprocess cross section:

$$Q^2 \frac{d\hat{\sigma}}{dQ^2}(eg \rightarrow eJ/\psi) = \frac{2\pi^2 e_c^2 \alpha_s \alpha^2}{m_c \hat{s}} \int \frac{dy}{y^2} \left\{ \frac{1 + (1 - y)^2}{y} \right. \\ \times \left[y \langle \mathcal{O}^{J/\psi}[^1S_0, \underline{8}] \rangle + \frac{\langle \mathcal{O}^{J/\psi}[^3P_0, \underline{8}] \rangle}{m_c^2} \frac{3Q^2 + 7(2m_c)^2}{\hat{s}} \right] \\ \left. - \frac{\langle \mathcal{O}^{J/\psi}[^3P_0, \underline{8}] \rangle}{m_c^2} \frac{8(2m_c)^2 Q^2}{\hat{s}^3} \right\} \delta(\hat{s}y - (4m_c^2 + Q^2)), \quad (13)$$

where $\sqrt{\hat{s}}$ is the subprocess center-of-mass energy, Q^2 is the negative invariant mass of the photon, and y is the momentum fraction of the J/ψ relative to the incoming electron. To obtain the cross section one convolutes the expression given in eq.(13) with the gluon distribution function. The hadronization of the $c\bar{c}$ pair, produced initially in a color-octet state with spin/angular-momentum quantum numbers $^{2S+1}L_J$, into a J/ψ bound state is parametrized by the NRQCD matrix elements $\langle \mathcal{O}^{J/\psi}[^1S_0, \underline{8}] \rangle$ and $\langle \mathcal{O}^{J/\psi}[^3P_0, \underline{8}] \rangle$. Note that it is precisely the matrix elements appearing in eq.(13) that are at the heart of the discrepancy between the CDF measurement and the photoproduction results.

There is an important point regarding the differential cross section presented in eq.(13). In principle this result is valid for all values of Q^2 , however, there are corrections due to higher twist terms that have been neglected in the derivation of the factored form of the cross section. These higher twist terms are suppressed by powers of m_c^2/Q^2 , and will, therefore, vanish for $Q^2 \gg m_c^2$. Thus it is necessary to compare the theoretical results presented in eq.(13) to experimental data in the large Q^2 regime. In the limit where $\hat{s}, Q^2 \gg m_c^2$, eq.(13) reduces to

$$\lim_{\hat{s}, Q^2 \gg m_c^2} Q^2 \frac{d\hat{\sigma}}{dQ^2}(eg \rightarrow eJ/\psi) \rightarrow \frac{2\pi^2 e_c^2 \alpha_s \alpha^2}{m_c \hat{s}} \int dy \frac{1 + (1 - y)^2}{y^2} \\ \times \left\{ \langle \mathcal{O}^{J/\psi}[^1S_0, \underline{8}] \rangle + 3 \frac{\langle \mathcal{O}^{J/\psi}[^3P_0, \underline{8}] \rangle}{m_c^2} \right\} \delta(y - \frac{Q^2}{\hat{s}}). \quad (14)$$

Note that for large Q^2 the linear combination $\langle \mathcal{O}^{J/\psi}[^1S_0, \underline{8}] \rangle + 3\langle \mathcal{O}^{J/\psi}[^3P_0, \underline{8}] \rangle/m_c^2$ is determined. This is precisely the linear combination of NRQCD matrix elements that is

measured at CDF. Therefore J/ψ lepto-production can provide an independent means of determining this linear combination of NRQCD matrix elements in a manner different from the CDF measurement.

Currently there exists experimental data on the production of J/ψ in μN collisions [33], however, the values of Q^2 probed in this experiment are too low to be in the asymptotic region, and the error on the experimental measurements are too large to allow for an accurate determination of the color-octet matrix elements. The high-statistics measurements to be expected in the future at HERA could definitely help to improve the situation and to constrain the color-octet matrix elements.

8 Conclusion

We have worked out and reviewed the impact of color-octet contributions on quarkonium production in photon-proton collisions and deep-inelastic scattering at HERA. Photo-production of J/ψ , ψ' , Υ and χ states, associated $J/\psi + \gamma$ production, fragmentation and resolved-photon contributions as well as deep inelastic J/ψ production have been discussed. We have shown how these reactions can be used to constrain the color-octet matrix elements and test the picture of quarkonium production as developed in the context of the NRQCD factorization approach.

Acknowledgements

Numerous and fruitful conversations with Mario Greco are gratefully acknowledged. Section 7 was prepared in collaboration with Sean Fleming. We are grateful to him and to Rohini Godbole and K. Sridhar for providing Figure 3 at short notice.

References

- [1] H. Jung, G.A. Schuler and J. Terrón, Proc. ‘Physics at HERA’, Eds. W. Buchmüller, G. Ingelman, DESY, Hamburg, 1992 and Int. J. Mod. Phys. A7 (1992) 7955; A. Ali, Proceedings, ‘XXI International Meeting on Fundamental Physics’, Madrid, 1993.
- [2] E.L. Berger and D. Jones, Phys. Rev. **D23** (1981) 1521; R. Baier and R. Rückl, Phys. Lett. **102B** (1981) 364; J.G. Körner, J. Cleymans, M. Kuroda and G.J. Gounaris, Nucl. Phys. **B204** (1982) 6; R. Baier and R. Rückl, Nucl. Phys. **B208** (1982) 381, *ibid.* B218 (1983) 289, Z. Phys. **C19** (1983) 251; for a recent review see also G.A. Schuler, CERN-TH.7170/94 (hep-ph/9403387).

- [3] H. Fritzsch, Phys. Lett. **B67** (1977) 217; H. Fritzsch and K.H. Streng, Phys. Lett. **B72** (1978) 385; M. Glück, J.F. Owens and E. Reya, Phys. Rev. **D17** (1978) 2324; for a recent work see J.F. Amundson, O.J.P. Eboli, E.M. Gregores and F. Halzen, MADPH-96-942 (hep-ph/9605295).
- [4] G.T. Bodwin, E. Braaten and G.P. Lepage, Phys. Rev. **D51** (1995) 1125.
- [5] W.E. Caswell and G.P. Lepage, Phys. Lett. **B167** (1986) 437.
- [6] G.P. Lepage, L. Magnea, C. Nakhleh, U. Magnea and K. Hornbostel, Phys. Rev. **D46** (1992) 4052.
- [7] E. Braaten and S. Fleming, Phys. Rev. Lett. **74** (1995) 3327; M. Cacciari, M. Greco, M.L. Mangano and A. Petrelli, Phys. Lett. **B356** (1995) 560.
- [8] P. Cho and A.K. Leibovich, Phys. Rev. **D53** (1996) 150 and *ibid.* **53** (1996) 6203.
- [9] E. Braaten and Y.-Q. Chen, Phys. Rev. Lett. **76** (1996) 730; K. Cheung, W.-Y. Keung and T.C. Yuan, Phys. Rev. Lett. **76** (1996) 877; P. Cho, Phys. Lett. **B368** (1996) 171; W.-K. Tang and M. Vänttinen, Phys. Rev. **D53** (1996) 4851 and NORDITA-96-18-P (hep-ph/9603266); S. Fleming and I. Maksymyk, Phys. Rev. **D54** (1996) 3608; S. Gupta and K. Sridhar, TIFR-TH-96-04 (hep-ph/9601349); M. Beneke and I.Z. Rothstein, Phys. Rev. **D54** (1996) 2005; P. Ko, J. Lee and H.S. Song, Phys. Rev. **D53** (1996) 1409; S. Fleming, O.F. Hernández, I. Maksymyk, H. Nadeau, MADPH-96-953 (hep-ph/9608413).
- [10] W. Koepf, P.V. Landshoff, E.M. Levin and N.N. Nikolaev, Proc. ‘Future Physics at HERA’, Eds. A. de Roeck, G. Ingelman and R. Klanner, DESY, Hamburg, 1996 and references therein.
- [11] W.Y. Keung and I.J. Muzinich, Phys. Rev. **D27** (1983) 1518; H. Jung, D. Krücker, C. Greub and D. Wyler, Z. Phys. **C60** (1993) 721; H. Khan and P. Hoodbhoy Phys. Lett. **B382** (1996) 189.
- [12] M. Krämer, J. Zunft, J. Steegborn and P.M. Zerwas, Phys. Lett. **B348** (1995) 657.
- [13] M. Krämer, Nucl. Phys. **B459** (1996) 3.
- [14] M. Cacciari and M. Krämer, Phys. Rev. Lett. **76** (1996) 4128.
- [15] J. Amundson, S. Fleming and I. Maksymyk, UTTG-10-95 (hep-ph/9601298).
- [16] P. Ko, J. Lee and H.S. Song, SNUTP-95-116 (hep-ph/9602223).

- [17] E. Braaten, S. Fleming and T.C. Yuan, OHSTPY-HEP-T-96-001 (hep-ph/9602374), E. Braaten and Y.-Q. Chen, Phys. Rev. **D54** (1996) 3216.
- [18] S. Aid et al. [H1 Collab.], Nucl. Phys. **B472** (1996) 3.
- [19] M. Derrick et al. [ZEUS Collab.], presented by L. Stanco at the International Workshop on Deep Inelastic Scattering, Rome, April 1996.
- [20] M. Glück, E. Reya and A. Vogt, Z. Phys. **C67** (1995) 433; A.D. Martin, G. Roberts and W.J. Stirling, Phys. Lett. **B354** (1995) 155; H.L. Lai, J. Botts, J. Huston, J.G. Morfin, J.F. Owens, J.W. Qiu, W.K. Tung and H. Weerts, Phys. Rev. **D51** (1995) 4763.
- [21] A.D. Martin, R.G. Roberts and W.J. Stirling, Phys. Lett. **B306** (1993) 145.
- [22] M. Derrick et al. [ZEUS Collaboration], Phys. Lett. **B345** (1995) 576; S. Aid et al. [H1 Collaboration], Phys. Lett. **B354** (1995) 494.
- [23] For a compilation of data see G.A. Schuler in [2].
- [24] E. Braaten and T.C. Yuan, prl71931673; M. Cacciari and M. Greco, Phys. Rev. Lett. **73** (1994) 1586; E. Braaten, M.A. Doncheski, S. Fleming and M.L. Mangano, Phys. Lett. **B333** (1994) 548; D.P. Roy and K. Sridhar, Phys. Lett. **B339** (1994) 141.
- [25] E. Braaten and T.C. Yuan, Phys. Rev. **D50** (1994) 3176; Y.Q. Chen, Phys. Rev. **D48** (1993) 5181; T.C. Yuan, Phys. Rev. **D50** (1994) 5664.
- [26] R. Godbole, D.P. Roy and K. Sridhar, Phys. Lett. **B373** (1996) 328.
- [27] V.A. Saleev, Mod. Phys. Lett. **A9** (1994) 1083.
- [28] G.T. Bodwin, E. Braaten and G.P. Lepage, Phys. Rev. **D46** (1992) R1914.
- [29] J.P. Ma, Nucl. Phys. **B460** (1996) 109.
- [30] M. Cacciari, M. Greco and M. Krämer, DESY 96-147.
- [31] C.S. Kim and E. Reya, Phys. Lett. **B300** (1993) 298.
- [32] S. Fleming, I. Maksymyk and T. Mehen, talk presented at the workshop ‘Quarkonium Physics’, Chicago, USA, June 13-15, 1996 and publication in preparation.
- [33] J.J. Aubert et al., Nucl. Phys. **B213** (1983) 1, Z. Phys. **C56** (1992) 21; D. Allasia et al., Phys. Lett. **B258** (1991) 493.